

SOME APPROXIMATIONS TO THE FLAPPING STABILITY OF HELICOPTER ROTORS

James C. Biggers
Research Scientist
Ames Research Center, NASA
Moffett Field, California 94035

Abstract

The flapping equation for a helicopter in forward flight has coefficients which are periodic in time, and this effect complicates the calculation of stability. This paper presents a constant coefficient approximation which will allow the use of all the well known methods for analyzing constant coefficient equations. The flapping equation is first transformed into the nonrotating coordinate frame, where some of the periodic coefficients are transformed into constant terms. The constant coefficient approximation is then made by using time averaged coefficients in the nonrotating frame. Stability calculations based on the approximation are compared to results from a theory which correctly includes all of the periodicity. The comparison indicates that the approximation is reasonably accurate at advance ratios up to 0.5.

to reduce computation effort and to gain insight into system behavior. However, for a helicopter in forward flight, the rotor flapping motion is described by a differential equation having coefficients which are periodic in time (azimuth). This fact complicates the solution of the equation, requiring methods which use considerable numerical computation and which give little insight. Thus it is desirable to find a differential equation with constant coefficients (hence an approximation) which adequately represents the forward flight flapping dynamics of a helicopter rotor. If such an equation is found, all of the well known techniques for analyzing constant coefficient equations may be used.

Notation

| | |
|------------------|---|
| a | blade lift curve slope |
| B | tip loss factor |
| c | blade chord |
| I | blade flapping inertia |
| i | $\sqrt{-1}$ |
| k_B | flapping spring stiffness |
| N | number of blades |
| R | rotor radius |
| t | time, sec |
| V | forward velocity |
| α | angle of attack of hub plane |
| β_i | flapping of ith blade relative to hub plane |
| $\vec{\beta}$ | vector of rotor degrees of freedom in nonrotating coordinates |
| β_0 | rotor coning angle |
| β_{1c} | rotor tilt forward (longitudinal flapping) |
| β_{1s} | rotor tilt to left (lateral flapping) |
| β_2 | rotor differential flapping |
| γ | blade lock number, $\rho ac R^4 / I$ |
| λ | eigenvalue or root, nondimensionalized by Ω , $\frac{\sigma}{\Omega} + j \frac{\omega}{\Omega}$ |
| μ | rotor advance ratio, $V (\cos \alpha) / \Omega R$ |
| ν | flapping natural frequency of rotating blade |
| σ | real part of eigenvalue |
| ρ | air density |
| ψ | azimuth angle, Ωt |
| Ω | rotor rotational speed |
| ω | imaginary part of eigenvalue |
| ω_B | flapping natural frequency of stationary blade, $\sqrt{k_B / I}$ |
| $(\dot{\quad})$ | derivative, $d(\quad) / d\psi$ |
| $(\ddot{\quad})$ | derivative, $d^2(\quad) / d\psi^2$ |

The flapping equation may be transformed into the nonrotating coordinate frame, as done in References 1 and 2, where some of the periodicity is transformed into constant terms. This result suggests that the use of constant coefficients in the nonrotating frame will retain some of the periodic system behavior. The constant coefficient approximation examined herein is made by using time averaged coefficients in the nonrotating frame. A comparison is made between the eigenvalues (stability) obtained from the approximation and the results from a theory which correctly includes all of the periodicity. The comparison indicates that the approximation is a useful representation of helicopter flapping dynamics for both hingeless and articulated rotors. This approximation was briefly discussed in Reference 1 for one set of rotor parameters. The present paper discusses the approximation in a more general manner and gives more insight into its features, limits, and applicability.

The rotor math model used here is for fixed shaft operation and includes only first mode (rigid blade) flapping, with spring-restrained flapping hinges at the hub center. Flapping natural frequency may be matched by selecting the spring rate. Thus the only approximations are in the use of the aerodynamic terms for rigid blade motion. Uniform inflow is used, and for the advance ratios considered here ($\mu < 0.5$), reverse flow effects are not included.

Equations of Motion

In this section, the single blade homogeneous flapping equation is presented for a rigid, spring-restrained, centrally hinged blade. This equation is then transformed to a nonrotating coordinate frame, using a coordinate transformation which is briefly discussed. Insight into the fundamental behavior of the rotor is gained by examining the hovering ($\mu = 0$) eigenvalues of the equation in nonrotating coordinates.

For helicopter stability and control studies, it is desirable to use as simple a math model as possible while retaining reasonable accuracy, both

Presented at the AHS/NASA-Ames Specialists' Meeting on Rotorcraft Dynamics, February 13-15, 1974.

For the single blade, the homogeneous equation of motion is

$$\ddot{\beta}_i + M_{\beta} \dot{\beta}_i + (\nu^2 + M_{\beta}) \beta_i = 0 \quad (1)$$

where

$$M_{\beta} = \frac{\gamma}{8} B^4 + \mu \frac{\gamma}{6} B^3 \sin \psi_i$$

$$M_{\beta} = \mu \frac{\gamma}{6} B^3 \cos \psi_i + \mu^2 \frac{\gamma}{8} B^2 \sin 2\psi_i$$

$$\nu^2 = 1 + \frac{\omega_{\beta}^2}{\Omega^2} = 1 + \frac{k_{\beta}}{I\Omega^2}$$

Note that reverse flow has not been included here. Although it could be included, it would not significantly affect the results for $\mu < 0.5$, since the additional terms are fourth order in μ .

By a coordinate transformation of the Fourier type, the single blade equation may be written in terms of nonrotating coordinates. The transformation accounts for the motion of all blades, and the number of degrees of freedom is equal to the number of blades. For example, with a three-bladed rotor, the degrees of freedom are coning (all blades flapping together), rotor pitching (cosine ψ flapping), and rotor rolling (sine ψ flapping). Adding a fourth blade adds a differential flapping degree of freedom, where blades 1 and 3 flap in one direction while blades 2 and 4 flap in the other direction. This type of differential motion is a degree of freedom with rotors having any even number of blades. Adding more blades adds degrees of freedom which, in the nonrotating frame, warp the plane described by the sine ψ and cosine ψ flapping motion.

The coordinate for the single blade is β_i . For a three-bladed rotor, the corresponding nonrotating coordinates are

$$\vec{\beta} = \begin{pmatrix} \beta_0 \\ \beta_{1c} \\ \beta_{1s} \end{pmatrix}$$

where β_0 , β_{1c} , and β_{1s} are rotor coning, pitching, and rolling motions. For a four-bladed rotor,

$$\vec{\beta} = \begin{pmatrix} \beta_0 \\ \beta_{1c} \\ \beta_{1s} \\ \beta_2 \end{pmatrix}$$

where β_2 is the differential flapping motion discussed above.

In general, the blade degrees of freedom in the transformation are

$$\beta_0 = \frac{1}{N} \sum_{i=1}^N \beta_i$$

$$\beta_{nc} = \frac{2}{N} \sum_{i=1}^N \beta_i \cos n\psi_i$$

$$\beta_{ns} = \frac{2}{N} \sum_{i=1}^N \beta_i \sin n\psi_i$$

$$\beta_{\frac{N}{2}} = \frac{1}{N} \sum_{i=1}^N \beta_i (-1)^i, \quad N \text{ even only}$$

Then the motion of the i th blade is

$$\beta_i = \beta_0 + \sum_{n=1}^K (\beta_{nc} \cos n\psi_i + \beta_{ns} \sin n\psi_i) + \beta_{\frac{N}{2}} (-1)^i;$$

$$K = \begin{cases} \frac{1}{2} (N - 1), & N \text{ odd} \\ \frac{1}{2} (N - 2), & N \text{ even} \end{cases}$$

The equations of motion (that is, eq. (1)) must also be converted from a rotating to a nonrotating frame by a similar procedure. This process is accomplished by operating on the equations with the summation operators

$$\frac{1}{N} \sum_i (\dots), \quad \frac{2}{N} \sum_i (\dots) \cos n\psi_i,$$

$$\frac{2}{N} \sum_i (\dots) \sin n\psi_i, \quad \frac{1}{N} \sum_i (\dots) (-1)^i$$

This is virtually the same procedure used in Reference 1.

It may be seen that the transformation involves multiplication by $\sin \psi$, $\cos \psi$, $\sin 2\psi$, $\cos 2\psi$, etc. This changes some of the periodic terms of the equations in the rotating reference frame into constants (plus higher harmonics) due to products of periodic terms, and vice versa.

Performing the indicated operations for $N = 3$ yields the following equations for a three-bladed rotor.

$$\vec{\beta} \cdot \begin{bmatrix} \frac{\gamma}{8} B^4 & 0 & \mu \frac{\gamma}{12} B^3 \\ 0 & \frac{\gamma}{8} B^4 + \mu \frac{\gamma}{12} B^3 \sin 3\psi & 2 - \mu \frac{\gamma}{12} B^3 \cos 3\psi \\ \mu \frac{\gamma}{6} B^3 & -2 - \mu \frac{\gamma}{12} B^3 \cos 3\psi & \frac{\gamma}{8} B^4 - \mu \frac{\gamma}{12} B^3 \sin 3\psi \end{bmatrix} \vec{\beta} + \begin{bmatrix} \nu^2 & \mu^2 \frac{\gamma}{16} B^2 \sin 3\psi & -\mu^2 \frac{\gamma}{16} B^2 \cos 3\psi \\ \mu \frac{\gamma}{6} B^3 + \mu^2 \frac{\gamma}{6} B^2 \sin 3\psi & \nu^2 - 1 + \mu \frac{\gamma}{6} B^3 \cos 3\psi & \frac{\gamma}{8} (B^4 + \frac{1}{2} \mu^2 B^2) + \mu \frac{\gamma}{6} B^3 \sin 3\psi \\ -\mu^2 \frac{\gamma}{8} B^2 \cos 3\psi & -\frac{\gamma}{8} (B^4 - \frac{1}{2} \mu^2 B^2) + \mu \frac{\gamma}{6} B^3 \sin 3\psi & \nu^2 - 1 - \mu \frac{\gamma}{6} B^3 \cos 3\psi \end{bmatrix} \vec{\beta} = 0 \quad (2)$$

Similarly, operating as above with $N = 4$, the equations of a four-bladed rotor are obtained.

$$\ddot{\vec{\beta}} + \begin{bmatrix} \frac{\gamma}{8} B^4 & 0 & \frac{\gamma}{12} B^3 & 0 \\ 0 & \frac{\gamma}{8} B^4 & 2 & \frac{\gamma}{6} B^3 \sin 2\psi \\ \frac{\gamma}{6} B^3 & -2 & \frac{\gamma}{8} B^4 & -\frac{\gamma}{6} B^3 \cos 2\psi \\ 0 & \frac{\gamma}{12} B^3 \sin 2\psi & -\frac{\gamma}{12} B^3 \cos 2\psi & \frac{\gamma}{8} B^4 \end{bmatrix} \vec{\beta} = 0$$

$$+ \begin{bmatrix} \nu^2 & 0 & 0 & \nu^2 \frac{\gamma}{8} B^2 \sin 2\psi \\ \frac{\gamma}{6} B^3 & \nu^2 - 1 + \nu^2 \frac{\gamma}{16} B^2 \sin 4\psi & \frac{\gamma}{8} (B^4 + \frac{1}{2} \nu^2 B^2 - \frac{1}{2} B^2 \nu^2 \cos 4\psi) & \frac{\gamma}{6} B^3 \cos 2\psi \\ 0 & -\frac{\gamma}{8} (B^4 - \frac{1}{2} \nu^2 B^2 + \frac{1}{2} \nu^2 B^2 \cos 4\psi) & \nu^2 - 1 - \nu^2 \frac{\gamma}{16} B^2 \sin 4\psi & \frac{\gamma}{6} B^3 \sin 2\psi \\ \nu^2 \frac{\gamma}{8} B^2 \sin 2\psi & \frac{\gamma}{6} B^3 \cos 2\psi & \frac{\gamma}{6} B^3 \sin 2\psi & \nu^2 \end{bmatrix} \vec{\beta} = 0 \quad (3)$$

The three- and four-bladed rotors have similar behavior except for the terms which are periodic in ψ . The periodic terms are 3/rev for the three-bladed rotor, but are 2 and 4/rev for the four-bladed rotor.

The main advantage of the transformed equations is that it is easier to express the combined rotor and airframe motions because the rotor equations are now in a nonrotating reference frame and include the motions of all blades. Furthermore, rotor motions are more intuitively understood, since the degrees of freedom are those seen by an observer in or beside the helicopter.

In the nonrotating coordinates of equations (2) and (3), the equations are coupled by off-diagonal terms. Note however, these are actually independent blades (unless some sort of feedback is added) and the coupling is due to the coordinate transformation.

To gain understanding of these degrees of freedom, the hovering ($\mu = 0$) behavior is examined next. The hover equations for four blades are given below.

$$\ddot{\vec{\beta}} + \begin{bmatrix} \frac{\gamma}{8} B^4 & 0 & 0 & 0 \\ 0 & \frac{\gamma}{8} B^4 & 2 & 0 \\ 0 & -2 & \frac{\gamma}{8} B^4 & 0 \\ 0 & 0 & 0 & \frac{\gamma}{8} B^4 \end{bmatrix} \vec{\beta} + \begin{bmatrix} \nu^2 & 0 & 0 & 0 \\ 0 & \nu^2 - 1 & \frac{\gamma}{8} B^4 & 0 \\ 0 & -\frac{\gamma}{8} B^4 & \nu^2 - 1 & 0 \\ 0 & 0 & 0 & \nu^2 \end{bmatrix} \vec{\beta} = 0 \quad (4)$$

For three blades, the hovering equations are identical, except that the β_2 equation is then absent. The β_0 and β_2 equations at hover are completely uncoupled and are both identical to that of the single blade in rotating coordinates.

$$\ddot{\beta}_i + \frac{\gamma}{8} B^4 \beta_i + \nu^2 \beta_i = 0 \quad (1), \text{ for } \mu = 0$$

$$\left. \begin{aligned} \ddot{\beta}_0 + \frac{\gamma}{8} B^4 \beta_0 + \nu^2 \beta_0 &= 0 \\ \ddot{\beta}_2 + \frac{\gamma}{8} B^4 \beta_2 + \nu^2 \beta_2 &= 0 \end{aligned} \right\} \text{ from equation (4)}$$

Eigenvalues of these equations are easily calculated, and are shown on figure 1. These will be

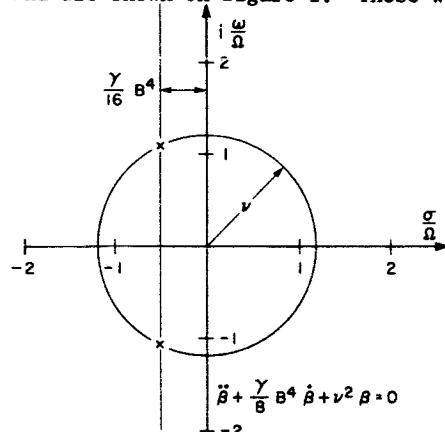


Figure 1. Hover eigenvalues of coning and reactionless modes ($\nu = 1.2$, $\gamma = 8$).

called coning and reactionless modes. The reactionless mode is so named because at hover it produces no net reaction at the hub. The equations for rotor pitching and rolling are,

$$\begin{pmatrix} \beta_{1c} \\ \beta_{1s} \end{pmatrix} + \begin{bmatrix} \frac{\gamma}{8} B^4 & 2 \\ -2 & \frac{\gamma}{8} B^4 \end{bmatrix} \begin{pmatrix} \beta_{1c} \\ \beta_{1s} \end{pmatrix} + \begin{bmatrix} \nu^2 - 1 & \frac{\gamma}{8} B^4 \\ -\frac{\gamma}{8} B^4 & \nu^2 - 1 \end{bmatrix} \begin{pmatrix} \beta_{1c} \\ \beta_{1s} \end{pmatrix} = 0$$

and the characteristic equation is then,

$$\left(\lambda^2 + \frac{\gamma}{8} B^4 \lambda + \nu^2 - 1 \right)^2 + \left(2\lambda + \frac{\gamma}{8} B^4 \right)^2 = 0$$

The eigenvalues for this equation are shown in figure 2. By analogy to a gyro, these modes will be called precession (the lower frequency mode) and nutation (the higher frequency mode). The damping, $-\gamma/16$, is the same as for the single blade of equation (1) and for the β_0 and β_2 modes discussed above. However, the coordinate transformation has resulted in the precession mode frequency being Ω lower than the single blade mode frequency in the

$$\begin{pmatrix} \beta_{1c} \\ \beta_{1s} \end{pmatrix}'' + \begin{bmatrix} \frac{\gamma}{8} B^4 & 2 \\ -2 & \frac{\gamma}{8} B^4 \end{bmatrix} \begin{pmatrix} \beta_{1c} \\ \beta_{1s} \end{pmatrix}' + \begin{bmatrix} \nu^2 - 1 & \frac{\gamma}{8} B^4 \\ -\frac{\gamma}{8} B^4 & \nu^2 - 1 \end{bmatrix} \begin{pmatrix} \beta_{1c} \\ \beta_{1s} \end{pmatrix} = 0$$

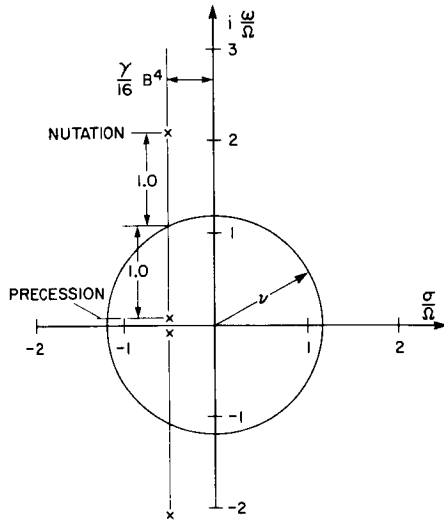


Figure 2. Hover eigenvalues of precession and nutation modes ($\nu = 1.2, \gamma = 8$).

rotating frame. Similarly, the nutation mode frequency is Ω higher than that of the single blade in the rotating frame.

The coning mode (fig. 1) will excite vertical motions of the vehicle, while the precession mode will excite pitch and roll motions. Thus vehicle responses are more intuitively understood by use of the nonrotating coordinates. Also, these equations may be used to study feedback control systems such as rotor tilting or rotor coning feedback, which were discussed in Reference 1. Note (from eqs. (1) and (2)) that the performance of such systems will depend on the number of blades used, since the blade motions become coupled by the feedback terms and the coupling will vary with the number of blades.

To compare the various modes with each other and with other theories, it is necessary to transform all eigenvalues into the same reference frame. The obvious choice is the rotating coordinates of equation (1), since most other theories are applicable to this frame. As may be seen by comparing figures 1 and 2, the precession and nutation modes may be transformed back into the rotating frame by adding and subtracting Ω respectively. This process results in four identical eigenvalues, as expected, since the rotor is composed of four identical blades, each described in the rotating frame by equation (1). As noted above, the frequencies of the β_0 and β_2 modes do not change

The equations for $\mu = 0$ have been easily solved and the nonrotating coordinate system has been presented and discussed. In nonhovering flight, however, the equations have periodic coefficients, which makes the equations more difficult to solve, as well as giving the solutions some special characteristics. These will be discussed in the next section.

Floquet Theory

Eigenvalues of equations such as (1) may be found with Floquet theory, as for example in References 3 and 4. The equation is integrated for one period ($\psi = 0, \dots, 2\pi$) for each independent initial condition to obtain the state transition matrix. The frequency and damping of the system modes are then obtained by taking the logarithms of the state transition matrix eigenvalues.

This technique has been applied here to three cases, and the results are shown on figure 3 for

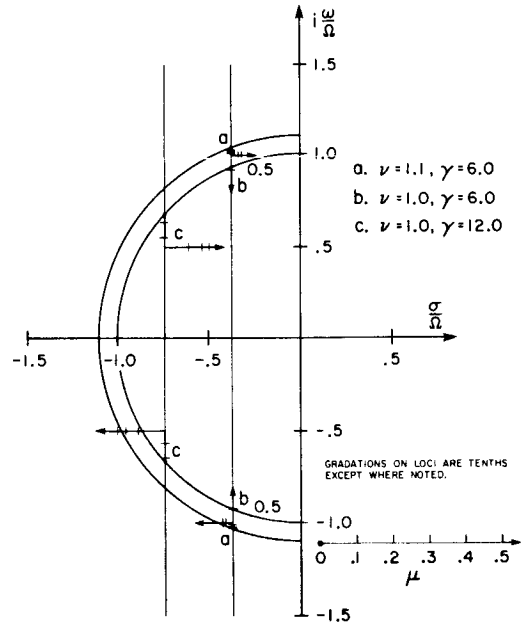


Figure 3. Floquet theory root loci for varying μ ; single blade in rotating coordinates.

varying μ . Note that as μ is increased, the frequency (ω/Ω) decreases, while the damping (σ/Ω) remains constant at $-\gamma/16$ until the frequency reaches an integer multiple of $1/2$ /rev. As μ is increased further, the frequency remains constant while the damping both decreases (the upper roots) and increases (the lower roots) as shown for cases a and c. This behavior may be surprising to those accustomed to constant coefficient equations, but is typical of periodic systems. The nonsymmetry about the real axis is analogous to the behavior of a constant coefficient equation root locus when the locus meets the real axis. At that point, the roots separate (no longer complex conjugates), one becoming less stable and the other becoming more stable. With periodic coefficient equations, the separation can occur at any multiple of $1/2$ the frequency of the periodicity. Actually, the constant coefficient equation is a special case of the periodic one, where the frequency in the coefficients is zero. This behavior may be seen in more detail by plotting the eigenvalues versus μ , as in figure 4, which again shows results from Floquet theory.

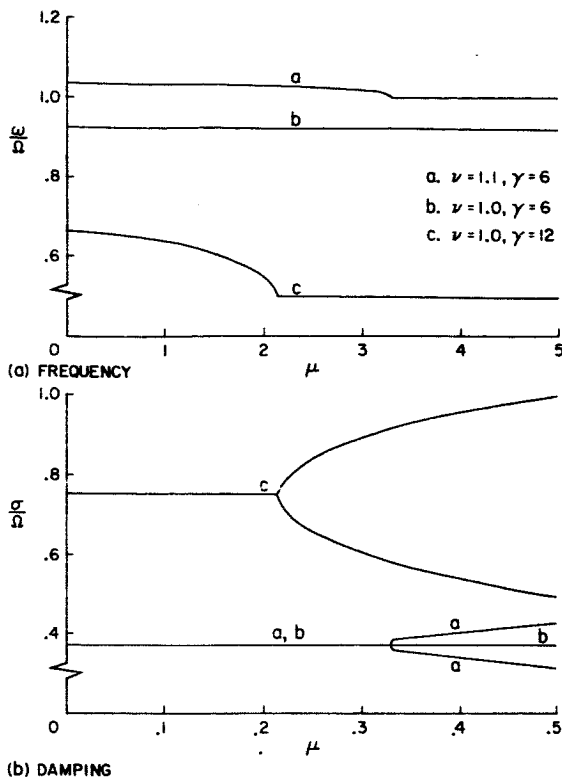


Figure 4. Floquet theory variation of frequency and damping with μ ; single blade in rotating coordinates.

Figures 3 and 4 have shown the eigenvalues in the rotating coordinate system. These may be transposed into the nonrotating system to examine the behavior of the nonrotating modes. Choosing case c ($\nu = 1.0, \gamma = 12$) as an example, the root locus is plotted on figure 5. The coning mode has the same eigenvalues shown in the two previous figures. The nutation and precession modes have the same damping, but as mentioned before, their frequencies are Ω higher and lower, respectively, than the coning frequency.

The regions where the frequency remains constant while the damping changes, called critical regions, may be illustrated by constructing the $\gamma - \mu$ plane as in figure 6 (and discussed in References 3 and 4). In the 0/rev region, the behavior is like that of a constant coefficient equation when the root locus meets the real axis; there are two real roots, with order μ^2 changes in damping. In the $1/2$ /rev region, the frequency is exactly half of the rotational frequency (fig. 3, case b), and the damping changes somewhat more rapidly. In the 1/rev region (fig. 3, case a) the frequency is the same as the rotational frequency (Ω), and again the damping changes are order μ^2 . As previously noted, damping is constant at $-\gamma/16$ outside of the critical regions. Note that varying ν has little effect on the boundaries of the 0/rev and $1/2$ /rev regions, but as ν is increased the 1/rev region moves upward.

In this section, the characteristics of the periodic coefficient solutions have been discussed

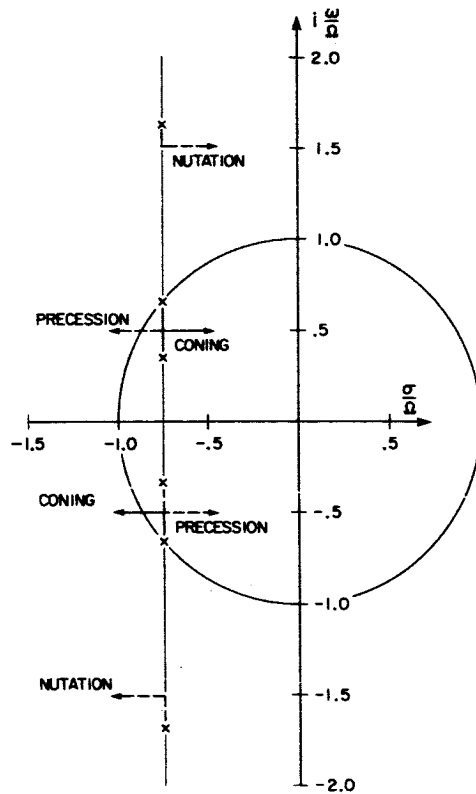
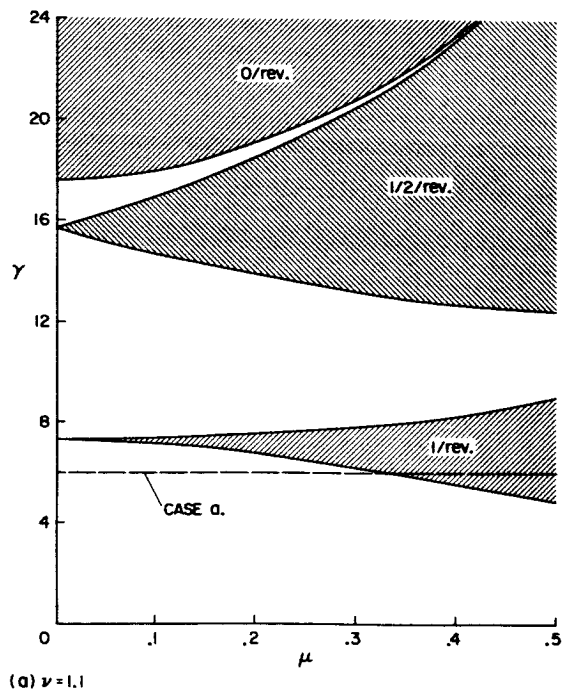


Figure 5. Floquet theory root loci for varying μ ; three-bladed rotor in nonrotating coordinates ($\nu = 1.0, \gamma = 12$; case c).



(a) $\nu = 1.1$

Figure 6. $\gamma - \mu$ plane for single blade in rotating coordinates based on Floquet theory.

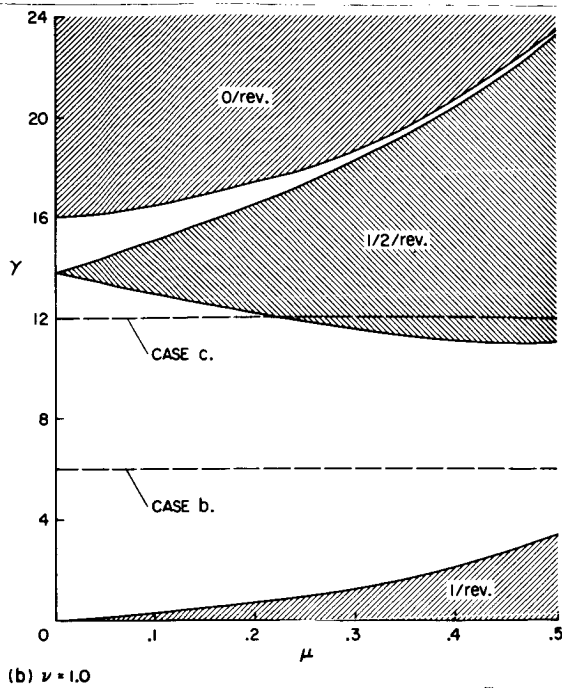


Figure 6. Concluded.

for nonhovering flight. The next sections will discuss an approximation which has constant coefficients, yet gives some of the behavior of the periodic coefficient system.

Constant Coefficient Approximation

In equation (1) the periodic coefficients are all of the speed (μ) dependent terms, and a constant coefficient approximation yields only the hover solution. However, in the nonrotating frame of equations (2) and (3), these periodic terms have been transformed into constants plus higher harmonic periodic terms. This result suggests that the primary effects of μ may be determined by using the average values of the coefficients. The constant coefficient approximation thus obtained for a four-bladed rotor is given in equation (5). The corresponding equation for three blades is identical, except that the β_2 motion is absent.

$$\begin{bmatrix} \frac{\gamma}{8} B^4 & 0 & \mu \frac{\gamma}{12} B^3 & 0 \\ 0 & \frac{\gamma}{8} B^4 & 2 & 0 \\ \mu \frac{\gamma}{6} B^3 & -2 & \frac{\gamma}{8} B^4 & 0 \\ 0 & 0 & 0 & \frac{\gamma}{8} B^4 \end{bmatrix} \vec{\beta} = 0$$

$$\begin{bmatrix} v^2 & 0 & 0 & 0 \\ \mu \frac{\gamma}{6} B^3 & v^2 - 1 & \frac{\gamma}{8} (B^4 + \frac{1}{2} \mu^2 B^2) & 0 \\ 0 & -\frac{\gamma}{8} (B^4 - \frac{1}{2} \mu^2 B^2) & v^2 - 1 & 0 \\ 0 & 0 & 0 & v^2 \end{bmatrix} \vec{\beta} = 0 \tag{5}$$

Note that the β_2 equation is not coupled to the others and is the same as the β_2 equation for hover; hence it yields only the $\mu = 0$ roots. Therefore the β_2 equation will not be discussed further or included in subsequent figures. The β_0 equation has only one μ -dependent term, coupling it to the β_{15} motion. The pitch and roll equations are coupled by both damping and aerodynamic spring terms.

Comparison

As noted earlier, eigenvalues may be compared by adding Ω to the precession frequency and subtracting Ω from the nutation frequency. In examining the constant coefficient approximation, any differences in eigenvalues will be due to the dropped periodicity. That is, all of the roots should approximate those obtained by using Floquet theory to solve equation (1). Using the comparison method mentioned above, the constant coefficient approximation is compared to Floquet theory results in figures 7, 8, and 9. The frequency scales have been expanded to exaggerate the effects of forward speed. Each of the three cases is discussed below.

Case a. $v = 1.1, \gamma = 6.$ (fig. 7)

This case corresponds to a hingeless rotor similar to the Lockheed XH-51. For this rotor the variations with μ of frequency and damping are small but significant since the 1/rev critical region is encountered (see fig. 6). All three modes of the approximation agree well with Floquet theory at low advance ratios, where the influence of the periodic coefficients is small. As the advance ratio is further increased, the precession mode displays the same type of behavior as the Floquet theory results, but the other two modes do not. For the precession mode (and the Floquet theory), the frequency becomes constant at 1/rev, and the damping then has two values as previously discussed. It is useful to examine why the constant coefficient approximation displays periodic

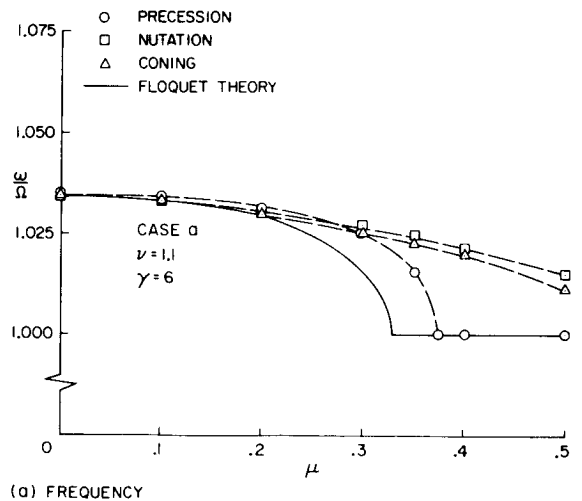


Figure 7. Comparison of constant coefficient approximation to Floquet theory ($v = 1.1, \gamma = 6$).

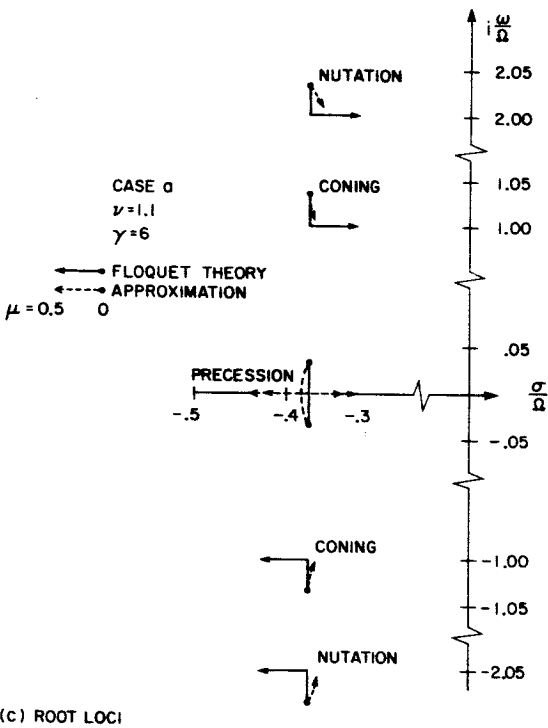
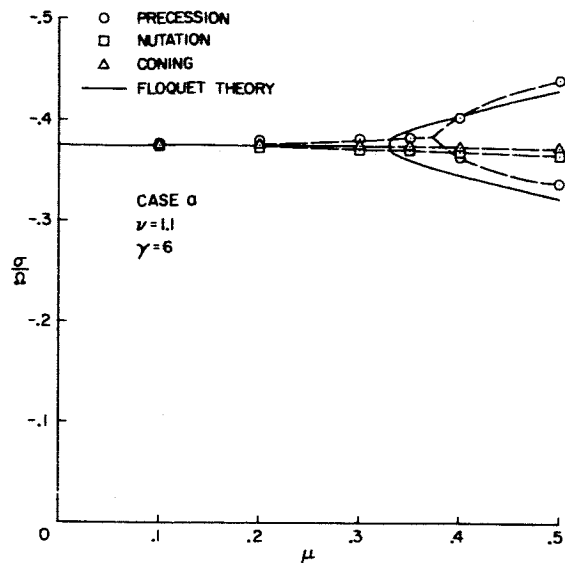


Figure 7. Concluded.

system (critical region) behavior. In this case, the precession roots at hover ($\mu = 0$) are very near the real axis due to the coordinate transformation. As μ is increased, the precession roots move toward the real axis and then split when they reach the axis, as usual with constant coefficient systems. Thus the damping both increases (the left branch) and decreases (the right branch).

Case b. $\nu = 1.0, \gamma = 6$. (fig. 8)

This case corresponds to an articulated rotor having relatively heavy blades, such as might be used for a high speed helicopter. This case is well removed from critical regions, and there are no significant changes in the eigenvalues for the μ range shown. The constant coefficient approximation agrees well with results from Floquet theory.

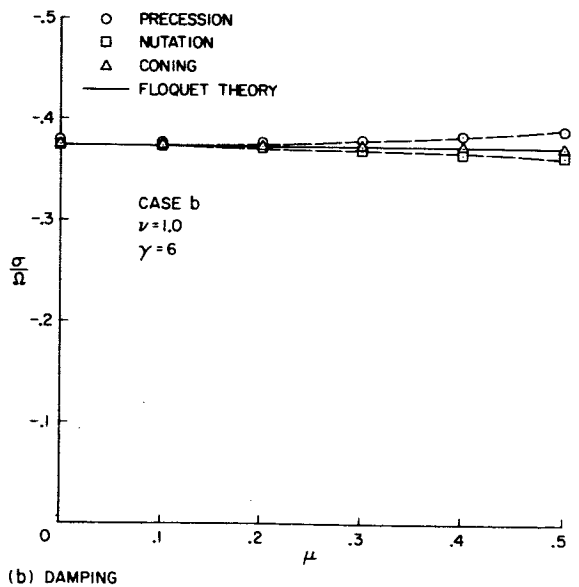
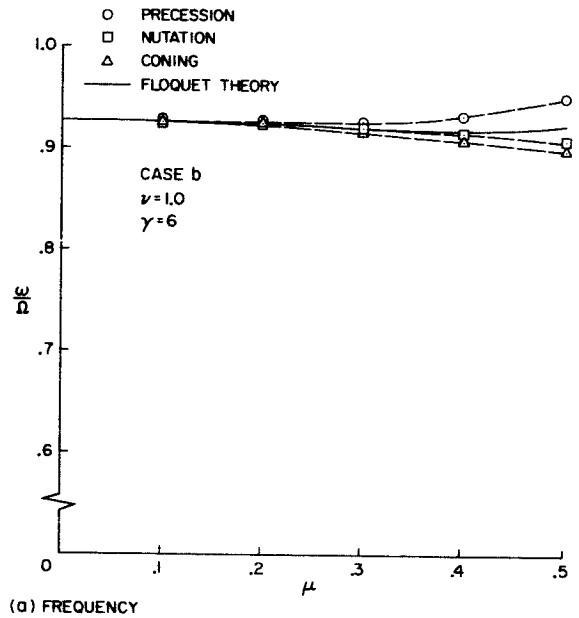
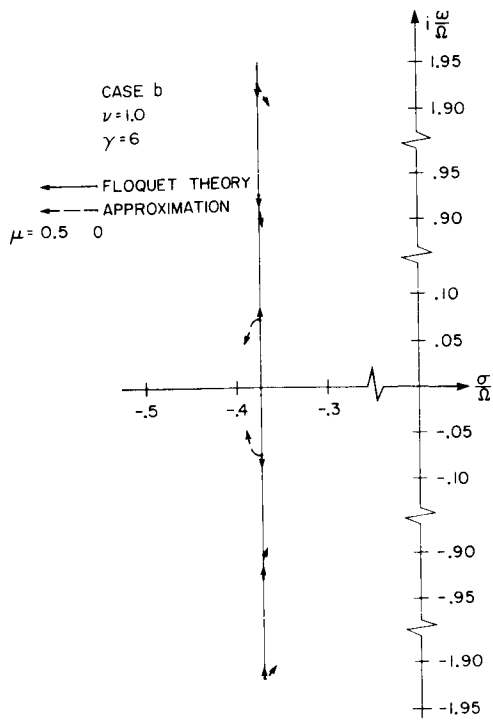
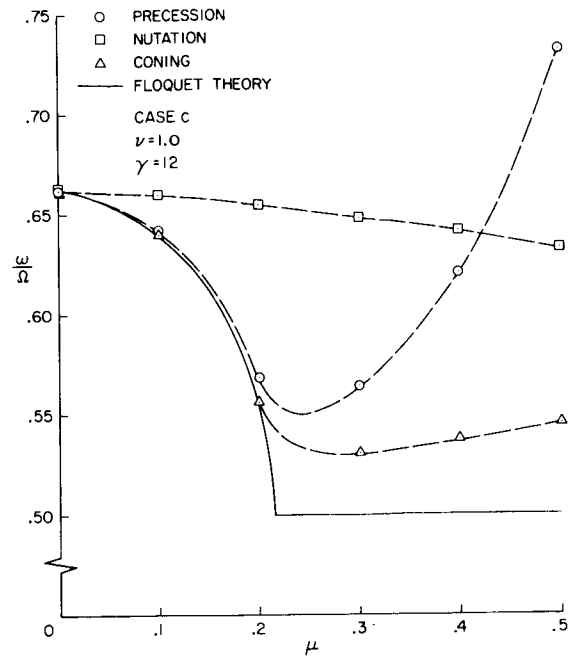


Figure 8. Comparison of constant coefficient approximation to Floquet theory ($\nu = 1.0, \gamma = 6$).



(c) ROOT LOCI

Figure 8. Concluded.



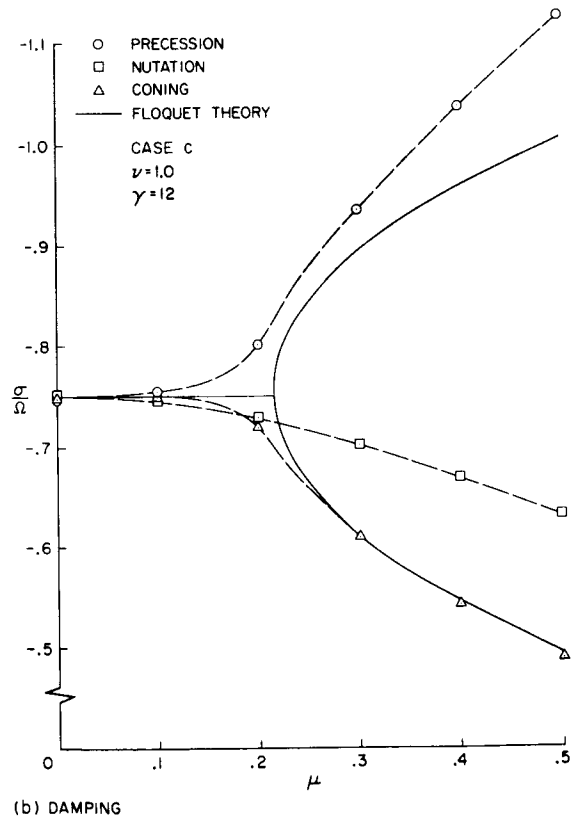
(d) FREQUENCY

Case c. $\nu = 1.0, \gamma = 12.$ (fig. 9)

This case corresponds to a typical articulated rotor with blades similar to many aircraft flying today. The Floquet theory indicates that the $\frac{1}{2}$ /rev region is encountered at $\mu = 0.215$. It is seen that the nutation mode is a poor approximation. Apparently, the constant coefficient approximation is not adequate for higher frequency modes if a critical region is encountered. The precession and coning modes (combined), however, do display the correct type of behavior: the frequency approaches $\frac{1}{2}$ /rev and the damping both increases (the precession mode) and decreases (the coning mode). In this case, the correct behavior is obtained because two modes are involved. As may be seen in figure 9(c), the two sets of Floquet roots approach each other, meet at $\frac{1}{2}$ /rev, and split (no longer complex conjugates). This behavior is approximated by the coning and precession modes, but in the approximation, the roots remain complex conjugates as shown in figure 9(c). The frequency of the precession mode does not agree well with Floquet results, but its damping is increasing; hence it is of less interest. The coning mode agrees well with the Floquet results, predicting the reduced damping very accurately.

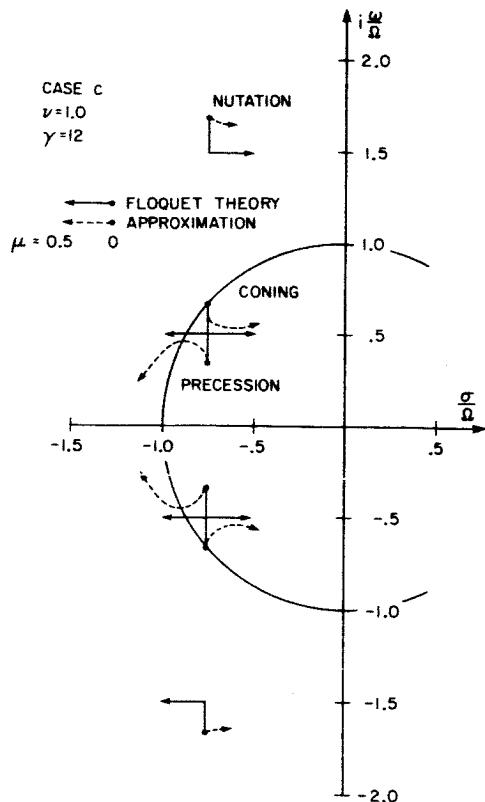
Perturbation Theory

Equation (1) has also been studied in Reference 5, using a perturbation technique known as the method of multiple time scales. Analytic expressions are derived for the eigenvalues, with expressions valid near and within each of the critical regions and ones which are valid away from the critical regions. These results are very



(b) DAMPING

Figure 9. Comparison of constant coefficient approximation to Floquet theory ($\nu = 1.0, \gamma = 12$).



(C) ROOT LOCI

Figure 9. Concluded.

useful; they give additional insight into the behavior of periodic systems in general and equation (1) in particular. A comparison between the Floquet results of the present work and the analytic results from Reference 5 indicates that the latter are also useful quantitatively. An exception is near the $\frac{1}{2}$ /rev region, where the perturbation solution was carried only to order μ . It should evidently be extended to order μ^2 as was the rest of the perturbation solution.

Discussion

Based on the cases described above, it is apparent that the constant coefficient approximation may be used to calculate rotor eigenvalues at advance ratios up to 0.5. A range of rotor parameters (γ and ν) have been studied which are representative of most conventional helicopters. The lower frequency modes agree well with Floquet results and display behavior approximating that of the Floquet theory critical regions. Therefore, there are many cases where the approximation may be used instead of more complicated methods.

The higher frequency modes of the approximation, however, do not display the correct behavior. Where these modes are important, for example, in using high gain feedback, the approximation should be used with caution.

The perturbation theory of Reference 5 is very easy to use for rotor stability calculations.

However, the solutions are for uncoupled blades in the rotating coordinate frame. To account for inter-blade coupling (as with certain feedback schemes) one must either use another technique such as that described herein or rederive the solutions with the coupling included.

Conclusion

Transforming the flapping equation of a helicopter rotor in forward flight into the nonrotating coordinate frame results in a set of differential equations where some of the periodicity due to forward flight is transformed into constant terms. Using the time-averaged values of these, i.e., dropping the remaining periodicity, gives a constant coefficient approximation which retains some of the periodic effects. Comparison between results of the approximation and those of Floquet theory indicates that the approximation should be acceptably accurate for calculating flapping stability of most helicopters for the advance ratios shown herein. Use of the nonrotating coordinates has given insight into rotor behavior and indicates how the vehicle motion would be affected by the rotor modes.

The higher frequency modes of the approximation do not agree well with Floquet theory. Where these modes are important for example, in using high gain feedback control systems, the approximation should be used with caution.

References

1. Hohenemser, K. H. and Yin, S-K., SOME APPLICATIONS OF THE METHOD OF MULTIBLADE COORDINATES, *Journal of the American Helicopter Society*, Vol. 17, No. 3, July 1972, pp 3-12.
2. NASA CR-114290, RESEARCH PROGRAM TO DETERMINE ROTOR RESPONSE CHARACTERISTICS AT HIGH ADVANCE RATIOS, Kuczynski, W. A. and Sissingh, G. J., February 1971.
3. Peters, D. A. and Hohenemser, K. H., APPLICATION OF THE FLOQUET TRANSITION MATRIX TO PROBLEMS OF LIFTING ROTOR STABILITY, *Journal of the American Helicopter Society*, Vol. 16, No. 2, April 1971, pp 25-33.
4. Hall, W. Earl Jr., APPLICATION OF FLOQUET THEORY TO THE ANALYSIS OF ROTARY-WING VTOL STABILITY, SUDAAR No. 400, Stanford University, February 1970.
5. NASA TM X-62,165, A PERTURBATION SOLUTION OF ROTOR FLAPPING STABILITY, Johnson, W., July 1972.